Chemical Shifts and Spin−Spin Coupling Constants in Me α-D-Xylopyranoside: A DFT Approach

O. L. Malkina,[†,⊥] M. Hricovíni,[‡] F. Bízik,[§] and V. G. Malkin*[,⊥]

Computing Center, Institute of Chemistry, Institute of Virology, Institute of Inorganic Chemistry, Slovak Academy of Sciences, SK-84236 Bratislava, Slovakia

Received: December 18, 2000; In Final Form: June 28, 2001

Chemical shieldings and coupling constants in a monosaccharide Me α- D-xylopyranoside were computed by density functional theory (DFT) method. The differences between the experimental and computed chemical shifts, for both DFT and MM3 geometries, showed that the method used reliably computes these NMR parameters. The agreement with experimental values was also obtained for proton−proton and proton−carbon coupling constants across one or more bonds. Furthermore, the effect of conformation upon both NMR shielding tensors (the values and orientation of its principal components) and couplings has also been investigated. The change of conformation around the C1−O1 linkage resulted in variations of mainly anomeric proton and carbon chemical shieldings as well as both the ring and O1 oxygens. The observed variations were found similar to those in Me β-D-xylopyranoside [Hricovíni, M.; Malkina, O. L.; Bízik, F; Turi Nagy, L.; Malkin, V. G. *J. Phys. Chem.* **1997**, *101*, 9756]. Similarly, the magnitudes of $^1J_{C-H}$ and $^3J_{C-H}$ varied upon the dihedral angle ϕ [H1−C1−O1−C_{Me}]. $^1J_{C1-H1}$ couplings, based on DFT geometry, changed between 151.7 and 165.6 Hz with the smallest values found for ϕ within −60° to 60°. $^3J_{H1-C1-O1-C_{Me}}$ varied between 0 and 11.2 Hz (DFT geometry) and showed the dependence comparable with the previous one for β anomer with one exception: the magnitude of $^3J_{C-H}$ for antiperiplanar conformation is about 3 Hz larger for the α anomer. Such differences could be important for the determination of glycosidic linkage conformation of carbohydrates and may suggest that this type of dependence should be parametrized separately for α- and β-linked carbohydrates.

Introduction

Determination of secondary and tertiary structure of biologically active molecules is often based on NMR spectral data in combination with computational methods. Chemical shifts and coupling constants are usually the primary parameters utilized in the initial step of an analysis. In most cases, the empirical rules are chosen for interpretation of shifts and couplings in terms of the structure parameters. However, recent advances in theory and computational methods now allow one to calculate the NMR parameters directly for a given structure.[1−10] Particularly interesting is the analysis of *J*-couplings and chemical shieldings in molecules possessing biological activity. Results of both ab initio and especially DFT methods[11−16] showed that the current methodology is capable of deriving the NMR parameters with high accuracy even in medium-sized molecules. Chemical shieldings and coupling constants exhibited a strong dependence upon the structure in various systems such as peptides[17−18] and carbohydrates.[19−25]

Recently, we have investigated the NMR shieldings and *J*-couplings in the monosaccharide Me β-D-xylopyranoside using the density functional theory (DFT) method.[21] We found that chemical shifts of anomeric proton, anomeric, and methyl carbon as well as the ring and O1 oxygens strongly depended on the dihedral angle ϕ. Similarly, the magnitudes of one- and three-bond proton−carbon coupling constants varied significantly due to stereoelectronic effects.[21] This agrees well with previous observations.[26,27] The present paper deals with the structurally similar monosaccharide, Me α-D-xylopyranoside (Scheme 1). The comparison with our previous study[21] of Me β-D-xylopyranoside allows us to examine which dependences of NMR parameters on the dihedral angle ϕ are similar for both monosaccharides and which are specific. The computed coupling constants and chemical shifts are compared with the previous data, and the effect of configuration and conformation upon the NMR parameters is discussed.

SCHEME 1

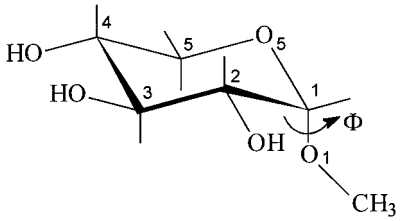

Methods

The DFT calculations have been carried out using a modified version of the deMon−KS program[28,29] augmented by the deMon−NMR code.[13] NMR chemical shifts were calculated using the sum-over-states density functional perturbation theory (SOS−DFPT).[12] The method employed for the calculation of

* E-mail: malkin@savba.sk. Fax: (421-2) 5941-0444. Telephone: (421-2) 5941-0469.
† Computing Center.
‡ Institute of Chemistry.
§ Institute of Virology.
⊥ Institute of Inorganic Chemistry.

10.1021/jp004530t CCC: $20.00
Published on Web 09/13/2001

TABLE 1: SOS−DFPT Computed Shielding Tensors[a] and the Experimental Chemical Shifts for Me α-D-Xylopyranoside

		computed					experimental	
atom		σ_{11}	σ_{22}	σ_{33}	σ_{iso}	δ_{iso}[b]	solution	solid-state[c]
C1	DFT	51.6	82.1	90.1	74.6	99.8	100.6	101.7
	MM3	47.7	76.1	87.1	70.3	99.6		100.3
C2	DFT	90.3	101.1	125.0	105.5	68.9	72.3	73.5
	MM3	86.1	95.1	116.6	99.3	70.6		72.6
C3	DFT	87.7	98.5	114.2	100.1	74.3	74.3	74.5
	MM3	81.6	96.7	108.5	95.6	74.3		74.5
C4	DFT	91.7	94.4	135.9	107.3	67.1	70.4	71.6
	MM3	86.9	92.2	129.5	102.9	67.0		69.8
C5	DFT	81.6	106.2	158.3	115.3	59.1	62.0	62.7
	MM3	80.5	104.3	158.9	114.6	55.3		61.7
O_{Me}	DFT	85.3	105.9	181.4	124.2	50.2	56.0	57.9
	MM3	86.5	103.5	181.3	123.8	46.1		55.4

[a] At the lowest energy minimum geometry calculated by DFT with TZVP basis and by MM3 method. [b] Referenced to the experimental value of C3. [c] See Taylor et al.[46] The resonance multiplicity is due to the inequivalence of two molecules in the asymmetric unit.

spin−spin coupling constant is described elsewhere.[11] All calculated couplings have been obtained with Perdew and Wang exchange[30] with Perdew correlation functional.[31] For chemical shift calculations, the Perdew and Wang exchange-correlation functional (PW91)[32] was used. The geometry was optimized with Becke exchange[33] and Perdew correlation functionals.[31] For calculations of couplings and chemical shifts, the basis set BIII of Kutzelnigg et al.[34] was used, and for the optimization of the structure, we used a smaller TZVP basis.[35] For comparison, the geometry was also optimized by the MM3 method with *MacroModel* V5.0.[36]

To study the dependence of NMR parameters on the dihedral angle ϕ [$\phi = \phi$ (H1−C1−O1− C_{Me})], the geometry was fully optimized (at the DFT level) with a fixed value of ϕ for different conformations ($\phi = 0, 30, 60, ..., 330°$).

The NMR spectra were collected on Bruker DPX 300 and AMX 500 MHz spectrometers in D_2O at 303 K. The chemical shifts are referenced to external TSP. The digital resolution of one-dimensional spectra was 0.1 Hz. The values of coupling constants were determined using the WINDAISY software for simulation of higher-order spin systems evaluating six spins within the system.

Results and Discussion

Chemical Shieldings and Coupling Constants Based on the Equilibrium Structure. We found that with both the DFT and MM3 methods the minimum energy for Me α-D-xylopyranoside corresponds to the angle $\phi \sim -52°$. The values of the computed isotropic chemical shieldings (σ_{iso}), the principal components of shielding tensor (σ_{ii}), based on these DFT and MM3 geometries, and the experimental shift values in solution and solid-state for Me α-D-xylopyranoside are listed in Table 1. The isotropic shieldings (σ_{iso}) of the ring carbons (C1 to C5) vary according to their position in the molecule, C1 being the most deshielded as expected. The same is valid for the principal components σ_{ii}. Until recently, the ^{13}C chemical shift tensors in carbohydrates were assumed to be axially symmetric. This general assumption was verified in the present study for Me α-D-xylopyranoside. The difference between the two closest principal components of the shielding tensor (σ_{ii}) for ring carbons can be relatively large, up to $\sim$ 50 ppm (see σ_{22} and σ_{33} for C5). For carbon in the OMe group, this difference is even larger (75.5 ppm). Thus, the shielding tensors cannot be considered as approximately axially symmetric except for C4 where $\sigma_{11} \sim \sigma_{22}$ for both DFT and MM3 geometries. Similar evidence found in β-anomer[21] might indicate the structural similarity of C4 environment in both α- and β-anomers. However, in structurally similar monosaccharides, Me α- and Me β-D-glucopyranosides, the measured σ_{ii} values in a single crystal also were found to be quite different for C4.[20] This experimental evidence could be due to the effect of the hydroxymethyl group in aldohexose molecules upon the local shielding at C4. In addition, the orientation of hydroxyl groups, predominantly at C4, can be different in solution and in solid-state. Since the present data were obtained for the isolated molecule, the effect of water molecules upon the formation of hydrogen bonds was neglected.

TABLE 2: Computed[a] and Experimental Coupling Constants (in Hz) for Me α-D-Xylopyranoside[b]

	DFT	MM3	experiment
$^1J_{C1H1}$	156.3 (156.6)[c]	167.3	170.1
$^1J_{C2H2}$	138.7	151.5	145.5
$^1J_{C5H5eq}$	141.9	148.3	
$^1J_{C5H5ax}$	133.2	134.6	
$^3J_{H1C_{Me}}$	4.4 (4.3)[c]	3.4	3.8
$^3J_{H1C3}$	4.3	3.9	
$^3J_{H1C5}$	8.0	7.1	
$^3J_{H5eqC1}$	9.2	9.7	
$^3J_{H5axC1}$	1.9	2.7	
$^2J_{H1C2}$	−0.4	0.0	
$^2J_{H2C1}$	−0.2	1.2	
$^3J_{H1H2}$	3.9	3.2	3.7
$^3J_{H2H3}$	8.7	7.8	9.6
$^3J_{H4H5eq}$	5.3	5.0	4.8
$^3J_{H4H5ax}$	10.5	10.4	10.9
$^2J_{H5axH5eq}$	−9.0	−10.0	−11.1

[a] At the lowest energy minimum geometry calculated by DFT with TZVP basis and by MM3 method. [b] Experimental couplings were obtained by computer simulation of the spin system. [c] Values in parentheses are averages as estimated using the three lowest minima. For all other listed couplings the effect was negligible.

The values of computed isotropic shifts (δ_{iso}, referenced to C3) for the DFT geometries are in agreement with the experimental values, though the discrepancies are slightly larger than those observed for the ring carbons in β-anomer.[21] The use of MM3 geometries leads to quite close results for the ring carbons, with a somewhat larger difference (3.8 ppm) for C5. The largest deviation from experiment was obtained for methyl carbon (5.8 and 9.9 ppm for DFT and MM3 geometries, respectively). That can be attributed to the above-mentioned neglect of the solvent effect as well as to the contribution of other low-energy conformers.

The experimental and the computed proton−proton ($^nJ_{H-H}$) and proton−carbon ($^nJ_{C-H}$) coupling constants are compared in Table 2. $^3J_{H-H}$ values match satisfactorily with the experimental coupling constants regardless of the method of geometry optimization, though these couplings based on DFT geometry are in slightly better agreement with the experimental values. For the geminal $^2J_{H5ax-H5eq}$, the picture is reversed: the difference between theory and experiment for the DFT geometry (2.1 Hz) is larger than for the MM3 one (1.1 Hz). Obviously, the reason for this disagreement lies in the different geometries obtained with DFT and MM3. The differences in the DFT and MM3 geometries also lead to different (up to 14 Hz) values of $^1J_{C-H}$ couplings. The latter indicates the high sensitivity of these spin−spin couplings to the structural parameters.

$^1J_{C1-H1}$ and $^1J_{C2-H2}$ computed couplings (DFT geometry) showed smaller values than the experimental ones, with a

TABLE 3: Energy[a] and Selected Geometrical Parameters Obtained by DFT (distances in Å) and MM3 for Different Conformers on the C1−O1 Linkage in Me α-D-Xylopyranoside

	DFT							MM3
angle	energy	C1O1	C1O5	C1H1	O5C1O1	C2C1O1	C1O1C$_{Me}$	C1H1
0	16.97	1.417	1.393	1.108	111.95	106.33	114.55	1.112
30	29.41	1.411	1.394	1.111	109.48	111.10	113.97	1.112
60	31.97	1.396	1.401	1.113	107.21	115.68	115.80	1.112
90	42.71	1.399	1.406	1.111	106.73	117.33	119.55	1.113
120	52.70	1.397	1.412	1.108	108.97	119.22	123.10	1.114
150	48.95	1.391	1.415	1.106	112.96	117.79	121.48	1.115
180	34.71	1.415	1.389	1.106	114.64	111.40	117.20	1.116
210	29.01	1.429	1.386	1.106	115.19	108.93	117.41	1.115
240	28.23	1.437	1.383	1.107	115.69	105.30	118.74	1.115
270	14.69	1.421	1.383	1.111	115.11	103.72	115.73	1.114
300	1.05	1.407	1.392	1.112	113.59	104.07	112.89	1.113
330	4.04	1.411	1.396	1.110	112.79	105.10	113.76	1.112

[a] ΔE in kJ/mol; energy minimum = −607.380 291 2 au at ϕ = 308°.

deviation of about 10%. This agrees with the results of Cloran et al.[23] for aldofuranosyl rings. The comparison of coupled-HF and DFT $^1J_{C-H}$ couplings computed in aldofuranosyl rings showed that the scaled HF couplings gave smaller values (up to ∼10 Hz) than those of the DFT-based couplings.[23] This evidence was explained by the inclusion of electron correlation in the DFT approach. Although better agreement with experiment was thus obtained by DFT, the calculated couplings were also systematically smaller than the measured $^1J_{C-H}$ as in our calculations for Me α-D-glucopyranoside. Rather surprisingly, better agreement in $^1J_{C-H}$ was found for MM3 than DFT geometry. For example, $^1J_{C1-H1}$ (MM3) is 167.3 Hz, which nearly corresponds to the experimental value (170.1 Hz), whereas the same DFT-based coupling is about 14 Hz lower. Similarly, $^1J_{C2-H2}$ (MM3) is closer to the experimental coupling than that based on the DFT geometry. This evidence is comparable to the results in the previous study of the related compound[21] and indicates that even this simple method for optimization of geometry yields the monosaccharide structure which is sufficient for calculation of coupling constants, all $^nJ_{H-H}$ and $^nJ_{C-H}$. Both geometries (DFT and MM3) allow correct interpretation of $^1J_{C-H}$ for axially and equatorially oriented C−H bonds. As the overlap between the lone-pair MO and the C−H bond is stronger in the synclinal position, $^1J_{C5-H5eq}$ becomes larger than $^1J_{C5-H5ax}$. Thus, the calculated $^1J_{C5-H5eq}$ > $^1J_{C5-H5ax}$ (141.9 and 133.2 Hz, respectively, for DFT geometry) and $^1J_{C1-H1}$ (α-anomer) > $^1J_{C1-H1}$ (β-anomer) (156.3 and 151.2 Hz, respectively, for DFT geometry).[21] Such evidence is important for the correct evaluation of configuration at the anomeric center and can complement the experimental data.[37,38]

The Fermi-contact term usually provides the main contribution to coupling constants. The PSO and the DSO terms in most cases compensate each other, resulting in their nearly negligible total magnitude. However, in some particular cases, such as long-range couplings, or in C−F couplings,[3] the sum of the PSO and the DSO may not be neglected. It is also noteworthy in this respect that the PSO and DSO contributions can vary in the magnitude and in the sign since they both strongly depend on the local electronic structure. Thus, the effect of oxygen lone pairs and the geometry of the array of atoms within the coupling pathway (and even nearby) may affect the spin−orbit contributions. Their absolute values can be up to ∼2.5 Hz, with opposite signs of the DSO and the PSO contributions. The sign changes when the stereochemistry of the array of atoms varies. For example, the contribution of the PSO is −0.79 Hz and the DSO is +0.78 Hz for $^3J_{H1-H2}$ in an α-anomer (the mutual H1 − H2 position is synclinal), whereas the contribution of the PSO is +2.12 Hz and the DSO is −2.20 Hz for the same coupling in a β-anomer (the H1 − H2 position is antiperiplanar). Similar changes in absolute values and signs were obtained for other couplings, such as $^3J_{H4-H5ax}$, $^3J_{H4-H5eq}$, $^3J_{C1-H5ax}$, $^3J_{C1-H5eq}$, supporting this stereoelectronic dependence of spin−orbit contributions.

Conformational Dependence of Chemical Shifts upon the Dihedral Angle ϕ. The effect of torsion (rotation around the C1−O1 linkage) upon the values of chemical shifts and coupling constants was studied. The computed energies and selected geometrical parameters as a function of dihedral angle ϕ are presented in Table 3. Remarkable variations in bond lengths and bond angles were obtained for various conformers. These changes are closely related to the stereoelectronic effects and therefore are closely connected with the changes of chemical shieldings and coupling constants. For example, C1−H1 bond length varied from 1.106 to 1.113 Å, being shorter for the antiperiplanar conformation. This change is in accord with the magnitude of computed $^1J_{C-H}$ where the larger coupling (see the discussion below) was found for the antiperiplanar conformation. The above finding agrees with the known relationship between the bond length (and consequently the s-character of the C−H bond) and the magnitude of $^1J_{C-H}$.[39] However, it contrasts with the recent evidence in 1,3 diheterocyclohexanes where no clear correlation between $^1J_{C-H}$ and bond lengths was observed.[40] The latter evidence might originate in simultaneous changes of the C1−O1 bond length and other geometrical parameters (the C1−O1 and C1−O5 distances, the O−C−O and C−O−C bond angles) that varied as a function of furanose ring conformation.[23] Consequently, the computed carbon−carbon and carbon−proton couplings changed with these geometrical parameters.

Both σ_{iso} and σ_{ii} depend considerably upon the ϕ dihedral angle (Table 4). The dependences of C1 and H1 shieldings are of primary interest due to their possible experimental applications. σ_{iso} of C1 varies from 71.3 to 80.4 ppm, being lower for syn conformations (Figure 1). Nearly constant values are obtained for ϕ within the interval 90° −270° (with a small minimum at about 180°) what is comparable with the finding in β-anomer. The range of variations of σ_{iso} of C1 is larger in the present case (∼9 ppm). However, the chemical shift difference between α and β anomers agrees well with the experimental trend. The analysis of the most important localized molecular orbital (LMO) contributions to the principal components shows (Table 5) their considerable stereochemical dependence as well as their partial compensation (especially at conformations within 90° − 270°). For example, contribution

TABLE 4: Effect of Torsion of ϕ Angle upon the Principal Components of Chemical Shielding Tensors (ppm) for Selected Atoms as Obtained by the SOS−DFPT Method for Me α-D-Xylopyranoside

	H-1				C-1				O-1			
ϕ	σ_{11}	σ_{22}	σ_{33}	σ_{iso}	σ_{11}	σ_{22}	σ_{33}	σ_{iso}	σ_{11}	σ_{22}	σ_{33}	σ_{iso}
0	23.5	26.4	29.3	26.4	46.1	77.0	91.8	71.6	231. 8	266.4	331.4	276.5
30	23.4	26.1	29.4	26.3	53.2	79.4	92.8	75.1	221. 6	268.0	326.6	272.1
60	23.8	24.3	30.2	26.1	58.2	78.1	96.3	77.5	232. 3	239.9	329.8	267.3
90	22.6	24.1	30.6	25.8	59.0	84.9	97.2	80.4	206. 8	255.5	347.3	269.9
120	22.0	24.6	30.4	25.7	53.7	89.9	97.7	80.4	187. 8	254.8	348.8	263.8
150	22.3	25.0	30.3	25.9	50.9	91.9	98.3	80.4	184. 7	256.6	319.8	253.7
180	22.3	24.7	30.7	25.9	46.7	88.3	99.8	78.3	204. 9	255.3	295.0	251.7
210	22.2	24.5	30.9	25.9	51.6	88.6	97.5	79.2	200. 5	264.5	331.8	265.6
240	22.1	24.7	31.1	26.0	57.3	87.5	95.5	80.1	189. 4	284.1	351.8	275.1
270	22.3	24.8	31.1	26.1	58.5	86.3	96.2	80.3	226. 3	265.6	332.4	274.8
300	23.0	25.3	30.9	26.4	53.1	84.7	91.3	76.4	238. 5	263.0	303.9	268.5
330	23.0	25.6	29.7	26.1	46.8	77.3	89.8	71.3	224. 9	266.6	311.3	267.6

	C_{Me}				O5				C2			
ϕ	σ_{11}	σ_{22}	σ_{33}	σ_{iso}	σ_{11}	σ_{22}	σ_{33}	σ_{iso}	σ_{11}	σ_{22}	σ_{33}	σ_{iso}
0	84.6	92.6	181. 9	119. 7	186. 7	262. 2	273. 3	240. 7	87.8	101.1	127.2	105.4
30	88.1	92.9	179. 4	120. 1	186. 4	256. 6	275. 1	239. 4	78.7	100.6	123.6	101.0
60	94.8	101. 0	174. 6	123. 5	190. 3	246. 6	281. 3	239. 4	81.1	97.5	123.0	100.5
90	97.6	106. 0	169. 1	124. 2	185. 8	242. 6	281. 7	236. 7	83.6	96.7	123.9	101.4
120	91.2	101. 3	170. 5	121. 0	177. 8	242. 3	279. 1	233. 1	85.7	95.0	124.5	101.7
150	85.0	99.6	169. 2	117. 9	159. 1	238. 9	274. 9	224. 3	88.5	94.2	127.6	103.4
180	95.8	102. 4	172. 2	123. 5	200. 5	247. 2	286. 3	244. 7	88.,2	101.3	125.3	104.9
210	95.0	110. 9	171. 6	125. 8	214. 6	257. 9	283. 8	252. 1	89.4	101.3	122.7	104.5
240	93.1	115. 4	178. 8	129. 1	220. 8	264. 9	271. 9	252. 5	89.9	100.2	121.7	103.9
270	96.1	111. 0	179. 1	128. 7	224. 5	261. 0	273. 3	252. 9	89.6	99.4.	122.0	103.7
300	89.1	108. 2	181. 0	126. 1	222. 7	265. 4	279. 3	255. 8	90.2	100.3	123.9	104.8
330	81.0	100. 4	181. 6	121. 0	202. 4	265. 3	275. 0	247. 6	89.4	101.7	127.0	106.0

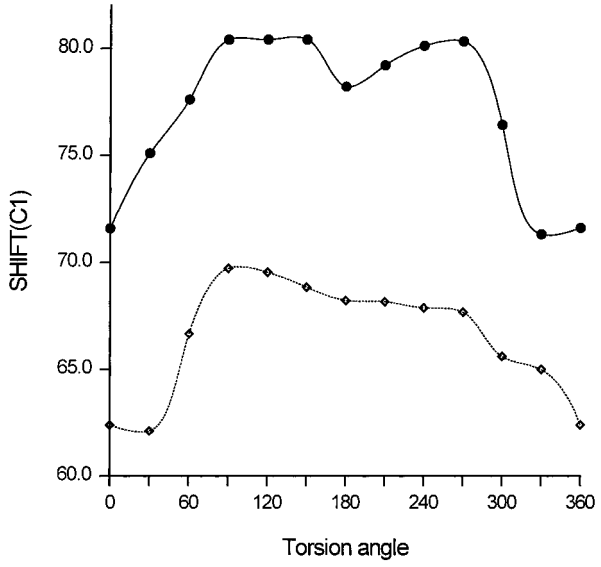

Figure 1. Dependence of the anomeric carbon (C1) shieldings (ppm) in Me α-D-xylopyranoside (dots, solid line) upon the dihedral angle ϕ (deg) as obtained by SOS-DFPT method. The same type of dependence for Me β-D-xylopyranoside (rhombuses, dotted line) is shown for comparison (taken from the previous study).

from LMO associated with the C1−O1 bond to both σ_{22} and σ_{33} of C1 showed strong dependence upon ϕ (up to ∼33 ppm). Although these variations in σ_{22} and σ_{33} partially compensate each other (resulting in overall smaller changes of σ_{iso} due to this bond) the LMO contribution to σ_{iso} gives shielded plateau at $\phi \sim 90°-150°$. On the other hand, the C1−H1 LMO contribution to σ_{11} and σ_{22} ranged up to ∼23 ppm. Their opposite trend in signs leads to the partial cancellation, too. The contribution of C1−H1 bond to σ_{iso} is shielded the most at $\phi \sim 270°-300°$. Thus, the observed dependence of C1 shielding is a curve with two maxima shifted by 120° (Figure 1), mainly defined by the contributions from LMOs of the bonds C1−O1 and C1−H1. This finding is very similar to that of our previous study.[21]

A strong conformation effect is also evident for σ_{iso} of H1 (Table 4, Figure 2). Chemical shieldings vary from 25.8 to 26.4 ppm with the smaller values observed for conformations at $\phi = 90°-240°$. This seems analogous to our previous results for the β-anomer where a strong effect of O1 lone pairs on shielding of H1 was discovered.[21] The same has been found in the present analysis: both lone pairs of O1 have the dominant effect upon σ_{iso} of H1. Contribution of the LMO of the first lone pair to σ_{iso} has minimum (−0.9 ppm) at 120°, whereas the LMO contribution of the second lone pair has minimum (−0.9 ppm) at 240° (data not shown). Thus, two minima are shifted by 120°. This phenomenon has a rather interesting consequence: the chemical shift of the anomeric proton of β anomer can be higher than the H1 shift for the α anomer for certain conformations (Figure 2). This differs from the situation discussed above for anomeric carbons where the α anomer carbon is always more shielded than the β one, regardless of conformation. To conclude, the considerable effect of conformation on both C1 and H1 shieldings in Me α-xylopyranoside is in agreement with our previous study[21] and supports the idea that stereochemical dependences of chemical shielding of anomeric proton and carbon could be useful in conformational analysis of oligosaccharides in solution and solid-state.

The strongest dependences of σ_{iso} on ϕ were found for O1 and O5 nuclei. For O1, the variations of σ_{iso} (25 ppm) are less pronounced than those found for the β-anomer (32 ppm),[21] whereas the range of changes of σ_{iso} of O5 is about 29 ppm (compare with 19 ppm in the β-anomer[21]). Both the effect of lone pairs of O1 and O5 oxygens as well as the influence of methyl carbon upon O5 shielding may partially explain these variations. Relatively strong mutual stereoelectronic interaction

TABLE 5: Contributions of Localized MO for Some Selected Bonds to σ Principal Components for Anomeric C1 as a Function of ϕ Torsion Angle

	C1−O1				C1−H1				C1−05			
ϕ	σ_{11}	σ_{22}	σ_{33}	σ_{iso}	σ_{11}	σ_{22}	σ_{33}	σ_{iso}	σ_{11}	σ_{22}	σ_{33}	σ_{iso}
0	−61.5	−3.5	−23.4	−29.5	−8.6	−37.5	−41.1	−29.1	−22.5	2.6	10.4	−3.2
30	−59.5	−10.6	−18.6	−29.5	−14.3	−30.0	−41.8	−28.7	−20.0	−6.8	17.6	−3.1
60	−53.5	−15.2	−13.0	−27.3	−15.9	−26.5	−42.2	−28.2	−17.5	−12. 7	21.2	−3.0
90	−53.7	−18.2	−7.0	−26.3	−5.1	−36.3	−42.2	−27.9	−18.5	−12. 2	20.3	−3.5
120	−53.4	−21.6	−2.8	−26.0	−1.1	−40.5	−42.4	−28.0	−21.9	−7.6	19.1	−3.4
150	−51.8	−27.0	2.4	−25.4	2.8	−45.2	−42.0	−28.2	−26.3	−12. 4	20.1	−6.2
180	−56.9	−32.8	3.5	−28.8	8.3	−48.1	−43.6	−27.8	−21.4	−11. 3	14.9	−5.9
210	−59.6	−33.2	5.0	−29.3	7.7	−48.2	−44.2	−28.2	−16.3	−11. 4	13.4	−4.8
240	−62.6	−29.6	3.5	−29.6	4.8	−46.4	−43.2	−28.3	−19.7	−6.7	−0.3	−4.5
270	−60.7	−26.1	−1.3	−29.3	−1.3	−40.4	−40.8	−27.5	−20.0	−5.4	13.8	−3.9
300	−58.0	−13.9	−14.9	−28.9	2.0	−39.0	−41.7	−27.6	−23.7	13.3	4.6	−2.0
330	−59.4	0.0	−27.3	−28.9	−5.0	−39.1	−42.2	−28.8	−24.1	17.8	2.9	−2.5

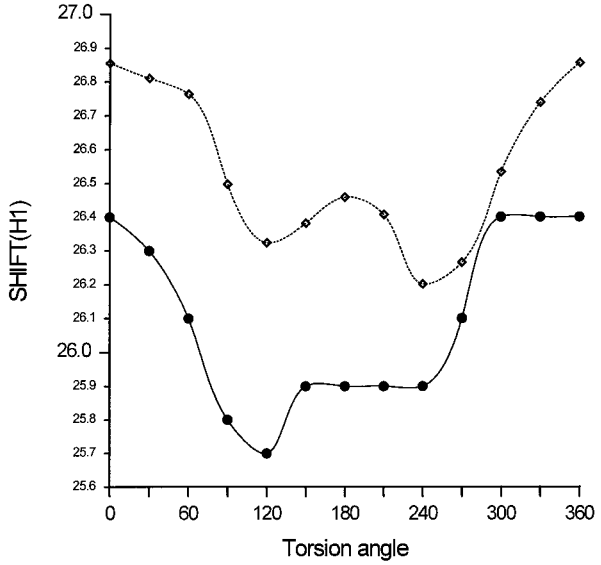

Figure 2. Dependence of the anomeric proton (H1) shieldings (ppm) in Me α-D-xylopyranoside (dots, solid line) upon the dihedral angle ϕ (deg) as obtained by SOS−DFPT method. The same type of dependence for Me β-D-xylopyranoside (rhombuses, dotted line) is shown for comparison (taken from the previous study).

between O1 and O5 pairs results in large variations of O5 and O1 shieldings. The overall σ_{iso} of O5 lone pairs vary up to 12 ppm and those at O1 up to 6 ppm.

Finally, σ_{iso} of C2 shows the dependence on the dihedral angle as well. This is influenced mainly by the O1 lone pairs and, when comparing to the β-anomer, by the axial orientation of C1−O1 bond. The above effects result in two minima of the chemical shift of C2 nucleus at $\phi \sim 60°$ and 270°. Interestingly, considerable shielding at C2 has been observed in the β-anomer at antiperiplanar conformation (the change ~ 12 ppm),[21] whereas the comparable σ_{iso} is obtained in the present case (within 1 ppm). For the α-anomer, the considerable deshielding effect was found for ± sc conformations.

It is also of interest to analyze the orientation of principal components of a chemical shielding (CS) tensor on an atom with respect to its bonds with neighboring atoms. In particular, let us consider how the directions of the principal components of the CS tensor on C1 change upon the rotation of the dihedral angle ϕ. One can expect that some components would keep preferable angles with certain bonds. It should be noted that the rotation upon ϕ slightly affects the bonding angles near C1. The σ_{11} component keeps a nearly constant angle (84.7 ± 5.1°) with the C1−O5 bond and approximately the same angle (83.7 ± 6.1°) with the C1−O1 bond. This means that this component is practically perpendicular to the O5−C1−O1 plane. σ_{11} also quite closely follows the C2−C1−H1 plane, with a maximal deviation of 18.3° (for the dihedral σ_{11}–C2−C1−H1 angle). The σ_{22} component almost lies in the O5−C1−O1 plane. The sum of angles σ_{22}–C1−O5 and σ_{22}–C1−O1 deviates from O5−C1−O1 angle by not more than 1.1° (this difference must be equal to zero if the component would lie exactly in the O5−C1−O1 plane). However, the direction of σ_{22} in this plane varies significantly: the angle σ_{22}–C1−O1 changes from 44.6 to 83.4° during the rotation. The σ_{33} component remains more or less perpendicular to the C1−H1 bond, making an angle of 85.1 ± 4.1°, whereas its angle with respect to the C1−C2 bond has a more significant deviation during the rotation (80.2 ± 9.4°). Approximately, one can say that this component is perpendicular to the C2−C1−H1 plane and it lies nearly in the O5−C1−O1 plane: the maximal deviation of the dihedral σ_{33}–O5−C1−O1 angle from zero is 18.3°. The contribution from a bond LMO to a principal component of the CS tensor is maximal when they are perpendicular to each other and it goes to zero as they become parallel (see elsewhere[34] for explanations and examples of analyses in terms of localized orbitals).

Thus, during the rotation, most of the changes in principle components of CS tensor are due to the change of the angles between the component and LMOs (in our case, bond LMOs). As a result, the total values of the principal components remain mostly unchanged due to compensation of contributions from different LMOs. However, such analysis gives an easy tool to access the preferable orientation of the principal components with respect to local bonds. The fact that a contribution (nonzero) of a bond LMO to a principal component of CS tensor almost does not change during the rotation indicates that the angle between this bond LMO and a component of the CS tensor is practically constant (see, for example, the almost constant contribution of C1−H1 LMO to σ_{33} on C1 listed in Table 5).

Conformational Dependence of Coupling Constants upon the Dihedral Angle ϕ. In carbohydrates, the computed $^1J_{C-H}$ indicated[21,23,24,26,27] that the values may vary up to 10−15 Hz, depending upon the torsion angle of the nuclei in the vicinity. The present analysis further supports this trend. For the DFT geometries, the difference between the smallest $^1J_{C-H}$ (151.7 Hz at $\phi = 30°$, Table 6) and the largest value (165.6 Hz at $\phi = 240°$) is nearly 14 Hz. Inspection of the shape of the $^1J_{C-H}$ dependence on the angle ϕ (Figure 3) indicates two maxima (at $\phi = 120°$ and 240°). This form is very similar to the dependence of H1 chemical shielding and again manifests the strong influence of oxygen lone pairs on one-bond coupling constants. The shape of this curve also is reminiscent of the dependence of chemical shielding upon the torsion angle in a β anomer (Figure 3 and elsewhere[21]). Further comparison of

TABLE 6: Effect of Torsion[a] upon the Computed $^1J_{C1-H1}$ and $^3J_{H1-CMe}$ (in Hz) in Me α-D-Xylopyranoside Based on Both DFT and MM3 Geometries

	$^1J_{C1-H1}$		$^3J_{H1-CMe}$	
ϕ	DFT	MM3	DFT	MM3
0	153.9	165.1	8.4	7.8
30	151.7	164.1	6.5	5.0
60	153.2	165.7	2.1	1.5
90	158.0	169.0	0	−0.1
120	162.0	173.7	3.3	3.4
150	162.0	176.6	9.4	9.0
180	161.9	174.9	11.2	11.3
210	163.1	173.0	7.4	7.1
240	165.6	172.2	2.2	1.3
270	161.8	170.7	0	0.3
300	157.6	167.3	3.1	3.2
330	155.3	165.3	6.8	6.5
360	153.9	165.1	8.4	7.8

[a] Rotation around the C1−O1 Linkage.

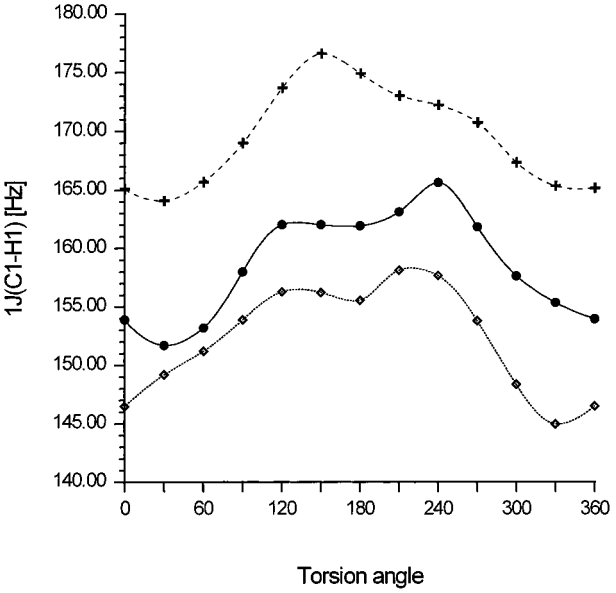

Figure 3. Dependence of the calculated one-bond proton−carbon coupling constant (in Hz) between anomeric carbon (C1) and proton (H1) upon the dihedral angle ϕ (deg) in Me α-D-xylopyranoside based on DFT (dots, solid line) and MM3 geometries (crosses, dashed line). The same type of dependence for Me β-D-xylopyranoside (rhombuses, dotted line) is shown for comparison (taken from the previous study).

$^1J_{C-H}$ in both anomers shows that $^1J_{C1-H1ax} > {}^1J_{Ca-H1eq}$ for certain conformations (Figure 3). For example, $^1J_{C1-H1ax}$ (β-anomer) = 156.2 Hz for $\phi = 150°$, and $^1J_{C1-H1eq}$ (α-anomer) = 151.7 Hz for $\phi = 30°$. Thus, the general rule proposed earlier ($^1J_{C1-H1ax} < {}^1J_{Ca-H1eq}$ of about 10 Hz)[38] may not be always valid. Actually, the violation of this rule ($^1J_{C1-H1ax} > {}^1J_{Ca-H1eq}$) was observed in azido sugars experimentally,[45] and now we present a firm theoretical support and explanation for this experimental finding. Therefore, straightforward application of that relationship in conformationally restricted (rigid) oligo- and polysaccharides, or their derivatives, may lead to an incorrect determination of anomeric configuration.

As mentioned previously, MM3 geometry for the lowest energy minimum yielded $^1J_{C1-H1}$ values closer to the experimental data than did the DFT geometries. The same is valid for the dihedral angle dependence of $^1J_{C1-H1}$ (Table 6 and Figure 3). The computed values of couplings varied from 164.1 to 176.6 Hz; that is they are about 10 Hz larger than DFT-based ones. In contrast to the curve obtained for the DFT geometry, no

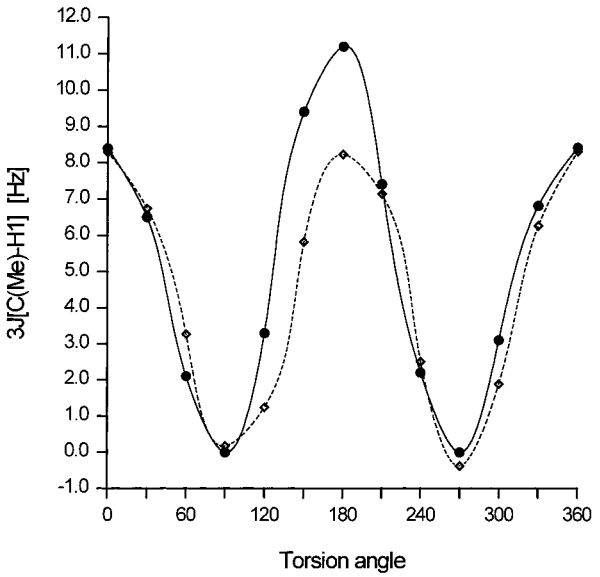

Figure 4. Dependence of the calculated three-bond proton-carbon coupling constant (in Hz) between anomeric carbon (C1) and proton (H1) upon the dihedral angle ϕ (deg) in Me α-D-xylopyranoside (dots, solid line). The same type of dependence for Me β-D-xylopyranoside (rhombuses, dotted line) is shown for comparison (taken from the previous study).

"irregularities" in the dependence of $^1J_{C1-H1}$ upon the torsion angle are observed for MM3 geometry. Furthermore, the largest $^1J_{C1-H1}$ value corresponds to $\phi = 150°$ with MM3 geometry, whereas for DFT geometry, the largest $^1J_{C1-H1}$ is obtained for $\phi = 240°$. Thus, geometries of two maxima calculated with MM3 are of lower quality than those of DFT. This evidence clearly indicates that the simple MM3 method cannot account for subtle stereoelectronic effects, such as the influence of oxygen lone pairs upon the geometry and, consequently, upon the magnitude of coupling constants. In any case, the present form of the $^1J_{C1-H1}$ dependence upon the ϕ angle supports the previous data and suggests the possibility of its application, as an additional constrain, in determination of the glycosidic linkage conformation in saccharides. For more quantitative application, however, further parametrization of the present dependence seems necessary.

The dependence of calculated three-bond proton-carbon coupling constants between H1 and C_{Me} ($^3J_{C-H}$) is presented in Table 6 as well. The magnitudes of $^3J_{C-H}$ vary significantly. For DFT geometries, the largest values are found for syn (8.4 Hz) and for anti conformation (11.2 Hz). Thus, the difference in $^3J_{C-H}$ for syn and anti conformations is nearly 3 Hz which is in good agreement with the experimentally parametrized $^3J_{C-H}$ curve.[43,44] $^3J_{C-H}$ values were also computed for MM3 geometries. The difference between DFT- and MM3-based couplings is 0.1 Hz (11.2 and 11.3 Hz, respectively) for $\phi = 180°$; the largest difference was obtained for $\phi = 30°$. However, the absolute computed values (for both geometries) for synclinal and antiperiplanar conformations are considerably higher (by about 3 Hz) with respect to the experimental data. This evidence seems similar to that found in the β-anomer. Since the conformationally rigid derivatives of monosaccharides have been used in the experimentally determined dependence of $^3J_{C-H}$[43] and the present theoretical data were obtained on Me α-xylopyranoside, the differences in chemical structures is one of the primary reasons for the above discrepancies. Also, as mentioned, the calculated coupling constants were obtained without solvent-effect evaluation. Finally, the DFT method itself can also be a

source of the differences (usually, DFT slightly underestimate calculated couplings), but this contribution should not be larger than 10%, judging by the data obtained for other couplings.

The most interesting result of the present calculation of $^3J_{C-H}$ is the difference between the magnitudes of $^3J_{C-H}$ for α- and β-linked carbohydrates (Figure 4). This difference is about 3 Hz for the antiperiplanar conformation ($\phi = 180°$) when $^3J_{C-H} = 11.2$ Hz for Me α-xylopyranoside and $^3J_{C-H} = 8.2$ Hz for Me β-xylopyranoside. This trend appears similar to the differences in $^1J_{C1-H1}$ where $^1J_{C1-H1ax} < {}^1J_{C1-H1eq}$ and it is the consequence of the effect of oxygen lone pairs in both anomers. Such subtle effect could not be observed in previous studies, based on semiempirical methods[26,27] as well as in experimental studies.[43,44] This might suggest that the Karplus-type relationship for $^3J_{C-O-C-H}$ should be parametrized separately for α- and β-linked carbohydrates to express more accurately the structural variations in different anomers.

Conclusions

In summary, the computed chemical shieldings and coupling constants in monosaccharide Me α-xylopyranoside confirm that reliable data can be obtained by quantum-chemical calculations with the DFT method. All computed ^{13}C chemical shifts were in good agreement with the experimental values, with a somewhat larger deviation obtained for carbon in the methyl group (likely due to limited flexibility of the group and the neglect of solvent effects in the calculations). Both proton−proton and proton−carbon coupling constants, across one or more bonds, also agreed with the measured couplings. The difference between $^1J_{C1-H1}$ in α and β anomers (as found in comparison with the data of previous work[21]) was 5.2 Hz for DFT-optimized geometry and ∼10 Hz for MM3-optimized geometry, which excellently corresponds to the experimental evidence (8.4 Hz). This trend, i.e., variations in one-bond proton-carbon couplings in axially or equatorially oriented C−H bonds, was easily seen also for $^1J_{C5-H5eq}$ and $^1J_{C5-H5ax}$ (141.9 and 133.2 Hz, respectively) on both experimental and theoretical levels. The conformational dependences of chemical shieldings support the idea that both anomeric proton and carbon values strongly depend on the dihedral angle ϕ and are in agreement with the data observed in β anomer.[21] The above variations are mostly defined by both O1 lone-pairs. The strong influence of conformation on the $^1J_{C1-H1}$ values is also in agreement with the evidence for the β anomer.[21] The comparison of both curves, in α and β anomers, indicates that $^1J_{C1-H1eq} < {}^1J_{C1-H1ax}$ only for certain conformations, and thus the anomeric configuration may not be always correctly determined solely from the magnitudes of $^1J_{C1-H1}$. Furthermore, the differences in $^3J_{C-H}$ in both anomers suggest that the Karplus-type relationship for $^3J_{C-O-C-H}$ should be parametrized separately for α- and β-linked carbohydrates to express more accurately the structural difference in these two classes of compounds. The orientation of the principal components of NMR shielding tensor during the rotation around the C1−O1 bond has been investigated. Analysis in terms of contributions from localized MOs associated with some bonds gives an easy tool to access the preferable orientation of the principal components with respect to local geometrical structure.

Acknowledgment. This work was supported by the Slovak Grant Agency VEGA (Grant Numbers 2/6037/99 and 2/7203/20), the Chemistry COST program (Project D9/0002/97). Computational resources of the Computing Center of the Slovak Academy of Sciences are gratefully acknowledged.

Supporting Information Available: Tables of angles on the C1 atom between the principal axes of NMR shielding tensor and the following: C1−O1, C1−C2, C1−H1, and C1−O5 LMOs. This material is available free of charge via the Internet at http://pubs.acs.orghttp://pubs.acs.org.

References and Notes

(1) Grant, D. M.; Facelli, J. C.; Alderman, D. W.; Sherwood, M. H. In *Nuclear Magnetic Shieldings and Molecular Structure*; Tossell, J. A., Ed.; Kluwer Academic Publishers: Dordrecht, 1993; p 367.

(2) Barfield, M. In *Nuclear Magnetic Shieldings and Molecular Structure*., Tossell, J. A., Eds.; Kluwer Academic Publishers: Dordrecht, 1993; p 523.

(3) Dickson, R. M.; Ziegler, T. *J. Phys. Chem.* **1996**, *100*, 5286.

(4) Rauhut, G.; Puyear, S.; Wolinski, K.; Pulay, P. *J. Phys. Chem.* **1996**, *100*, 6310.

(5) Forsyth, D. A.; Sebag, A. B. *J. Am. Chem. Soc.* **1997**, *119*, 9483.

(6) Tesche, B.; Haeberlen, U. *J. Magn. Reson. A* **1995**, *117*, 186.

(7) Tajkhorshid, E.; Paizs, B.; Suhai, S. *J. Phys. Chem. B.* **1997**, *101* 8021.

(8) Benedict, H.; Shenderovich, I. G.; Malkina, O. L.; Malkin, V. G.; Denisov, G. S.; Golubev, N. S.; Limbach, H.-H. *J. Am. Chem. Soc.* **2000**, *122*, 1979.

(9) Cornilescu, G.; Bax, A.; Case, D. A. *J. Am. Chem. Soc.* **2000**, *122*, 2168.

(10) Pearson, J. G.; Le, H.; Sanders, L. K.; Godbout, N.; Havlin, R. H.; Oldfield, E. *J. Am. Chem. Soc.* **1997**, *119*, 11941.

(11) Malkin, V. G.; Malkina, O. L.; Salahub, D. R. *Chem. Phys. Lett.* **1994**, *221*, 91.

(12) Malkin, V. G.; Malkina, O. L.; Casida, M. E.; Salahub, D. R. *J. Am. Chem. Soc.* **1994**, *116*, 5898.

(13) Malkin, V. G.; Malkina, O. L.; Eriksson, L. A.; Salahub, D. R. In *Modern Density Functional Theory: A Tool for Chemistry; Theoretical and Computational Chemistry*; Seminario, J. M., Politzer, P., Eds.; Elsevier: Amsterdam, 1995, Vol. 2.

(14) Malkina, O. L.; Salahub, D. R.; Malkin, V. G. *J. Chem. Phys.* **1996**, *105*, 8793.

(15) Malkin, V. G.; Malkina, O. L.; Steinebrunner, G.; Huber, H. *Chem. Eur. J.* **1996**, *2*, 452.

(16) Malkin, V. G.; Malkina, O. L.; Salahub, D. R. *J. Am. Chem. Soc.* **1995**, *117*, 3294.

(17) deDios, A. C.; Oldfield, E. *J. Am. Chem. Soc.* **1994**, *116*, 5307.

(18) deDios, A. C.; Pearson, J. G.; Oldfield, E. *J. Am. Chem. Soc.* **1993**, *115*, 9768.

(19) Dejaegere, A. P.; Case, D. A. *J. Phys. Chem. A* **1998**, *102*, 5280.

(20) Liu, F.; Phung, C. G.; Alderman, D. W.; Grant, D. M. *J. Am. Chem. Soc.* **1996**, 118, 10629.

(21) Hricovíni, M.; Malkina, O. L.; Bízik, F.; Turi Nagy, L.; Malkin, V. G. *J. Phys. Chem. A* **1997**, *101*, 9756.

(22) Bose, B.; Zhao, S.; Stenutz, R.; Cloran, F.; Bondo, P. B.; Bondo, G.; Hertz, B.; Carmichael, I.; Serianni, A. S. *J. Am. Chem. Soc.* **1998**, *120*, 11158.

(23) Cloran, F.; Carmichael, I.; Serianni, A. S. *J. Phys. Chem. A* **1999**, *103*, 3783.

(24) Church, T. J.; Carmichael, I.; Serianni, A. S. *J. Am. Chem. Soc.* **1997**, *119*, 8946.

(25) Cloran, F.; Carmichael, I.; Serianni, A. S. *J. Am. Chem. Soc.* **2000**, *122*, 396.

(26) Hricovíni, M.; Tvaroška, I. *Magn. Reson. Chem.* **1990**, *28*, 862.

(27) Tvaroška, I.; Taravel, F. R. *J. Biomol. NMR* **1992**, *2*, 421.

(28) Salahub, D. R.; Fournier, F.; Mlynarski, P.; Papai, I.; St-Amant, A.; Ushio, J. In *Density Functional Methods in Chemistry*; Labanowski, J. K., Andzelm, J. W., Eds.; Springer, New York, 1991; p 77.

(29) St-Amant, A.; Salahub, D. R. *Chem. Phys. Lett.* **1990**, *169*, 387.

(30) Perdew, J. P.; Wang, Y. *Phys. Rev* **1986**, *B 33*, 8800.

(31) Perdew, J. P.; *Phys. Rev.* **1986**, *B 33*, 8822; *34*, 7406.

(32) Perdew, J. P.; Wang, Y. *Phys. Rev.* **1992,** *B. 45*, 13244.

(33) Becke, A. D. *Phys. Rev.* **1988**, *A 38*, 3098.

(34) Kutzelnigg, W.; Fleischer, U.; Schindler, M. In *NMR: Basic Principles and Progress*:; Springer-Verlag: Heidelberg, 1990; Vol. 23, p 165.

(35) Godbout, N.; Salahub, D. R.; Andzelm, J.; Wimmer, E. *Can. J. Chem.* **1992**, *70*, 60.

(36) Mohamadi, F.; Richards, N. G. J.; Guida, W. C.; Liskamp, R.; Lipton, M.; Caufield, C.; Chang, G.; Hendrickson, T.; Still, W. C. *J. Comput. Chem.* **1990**, *11*, 440.

(37) Perlin, A. S.; Casu, B. *Tetrahedron Lett.* **1969**, 2921.

(38) Hansen, P. E. *Prog. NMR Spectrosc.* **1981**, *14*, 175.

(39) Gill, V. M. S.; Von Philipsborn, W. *Magn. Reson. Chem.* **1989**, *27*, 409.

(40) Cuevas, G.; Juaristi, E.; Vela, A. *J. Phys. Chem. A* **1999**, *103*, 932.
(41) Karplus, M. *J. Chem. Phys.* **1959**, *30*, 11.
(42) Egli H.; Von Philipsborn, W. *Helv. Chim. Acta*. **1981**, *64*, 976.
(43) Tvaroška, I.; Hricovíni, M.; Petrakova, E. *Carbohydr. Res.* **1989**, *189*, 359.
(44) Mulloy, B.; Frenkiel, T. A.; Davis, D. B. *Carbohydr. Res.* **1988**, *188*, 39.
(45) Szilágyi, L.; Györgydeak, Z. *Carbohydr. Res.* **1985**, *143*, 21.
(46) Taylor, M. G.; Marchessault, R. H.; Perez, S.; Stephenson, P. J.; Fyfe, C. A. *Can. J. Chem.* **1985**, *63*, 270.